

**Modeling composite electrolytes for low-temperature solid oxide fuel cells
application: structural, vibrational and electronic features of carbonate-oxide
interfaces**

-SUPPLEMENTARY INFORMATION-

Chiara Ricca¹, Andrey Grishin¹, Armelle Ringuedé¹, Michel Cassir¹, Carlo Adamo^{1,2}, and
Frédéric Labat^{1*}

¹*PSL Research University, Chimie Paristech-CNRS, Institut de Recherche de Chimie de
Paris, 11 rue Pierre et Marie Curie, F-75231 Paris Cedex 05, France*

²*Institut Universitaire de France, 103 Bd Saint-Michel, F-75005, Paris, France*

1. Building the YSZ-LiKCO₃ interface

1.1 A simple YSZ-LiKCO₃ interface model

The strategy followed to build the model of the YSZ-LiKCO₃ interface used in this work to simulate the composite material, starting from the available experimental data and the previously reported theoretical investigation of the isolated species is described here in details. Building the interface between chemically and structurally complex phases is a hard task, since different parameters, such as the coincidence of the lattice parameters and the initial surface configuration and orientation, should be taken into account. In the present case, we decided to start from the most stable surface of each phase we identified in our previous works on the oxide and carbonate phases.^{1,2}

Starting from experimental and theoretical evidences outlining that (111) is the most stable YSZ termination,³⁻⁶ the oxide model was built by cleaving the clean (111) surface of cubic ZrO₂ from the optimized bulk structure, considering only the most stable O terminated surfaces.⁴ To respect the neutrality of the system and to reproduce the experimental 8 mol% Y₂O₃ doping amount which provides stability and the highest experimental oxygen conductivity, a (2×2) supercell with a thickness of six slab layers (O-Zr-O) for a total of 72 atoms (Zr₂₄O₄₈), in which two oxygen vacancy were created and four Zr⁴⁺ ions of the supercell were replaced by four Y³⁺ cations has been considered. Moreover, in agreement with the observation of oxygen vacancy alignment along the [111] direction⁷, the two vacancies were placed along this direction, one at the top and one at the bottom of the supercell, with a distance of ~13 Å, hence avoiding spurious interaction between defects. Two Y atoms were then placed near each vacancy, both in next-nearest neighbour (NNN) positions to the vacancies (one Y on the outermost layer and the other in underneath one), which was found to be the most stable configuration. This optimized YSZ-(111) model, with a Zr₂₀Y₄O₄₆ stoichiometry and indicated as YSZ^{6L} in the following, has cell parameters $a=b=7.196$ Å, and $\gamma=120^\circ$. Further details can be found in ref 1.

LiKCO₃ has a monoclinic structure belonging to the P_{21/c} space group and has a layered nature, in which layers of LiO₅ distorted pyramids and KO₉ polyhedra of irregular shape are oriented parallel to the (10-1) direction and connected by distorted

but planar carbonate groups which are arranged perpendicularly to the c -axis. The most stable (001) surface was cut from the optimized LiKCO_3 bulk structure parallel to the (001) plane, obtaining a converged 3-layer thick slab model with cell parameters $a=7.254 \text{ \AA}$, $b=7.289 \text{ \AA}$, $\gamma=90^\circ$ for a total of 36 atoms with a $\text{Li}_6\text{K}_6(\text{CO}_3)_6$ stoichiometry. This surface model will be indicated in the following as $\text{LiKCO}_3^{3\text{L}}$.

The epitaxial constraints require a good coincidence of the lattice parameters of the two interacting surfaces, resulting in a strain free system. Unfortunately, while for the lattice parameters a and b of the aforementioned YSZ and LiKCO_3 models there is a moderate mismatch ($\delta_a=0.8\%$, $\delta_b=1.3\%$), a larger discrepancy is instead observed for the γ angle ($\delta_\gamma=33.3\%$). This would imply the necessity to consider larger unit cells together with the study of all resulting possible lattice coincidences that can be found at the interface between the two phases. Moreover, the YSZ supercell is oblique and, as observed by Bruno et al.⁸, in these cases, already with small angular mismatch, it is difficult having a good coincidence between the areas of the two surface lattices, because of the divergence of the lattice parameters when increasing the size of the supercell. Here, to reduce computational cost, instead of considering larger supercells to reduce lattice mismatch, we cut very large supercell models of the two surfaces ((4×4) for both the LiKCO_3 -(001) surface and the (2×2) supercell representing YSZ-(111)), and the carbonate slab was rotated of about 30° around the normal to the surface plane (see Figures S1a and S1b), so as to orient the CO_3 groups toward the Zr or Y surface sites. We then identified a new unit cell for the interphase (see Figure S1c) containing a number of atoms in line with the stoichiometry of each phase, thus ensuring the neutrality of the unit cell. The final unit cell has PI symmetry and contains 106 atoms, 36 ($\text{Li}_6\text{K}_6(\text{CO}_3)_6$) belonging to the 3 layers of the carbonate phase and 72 ($\text{Zr}_{20}\text{Y}_4\text{O}_{46}$) organized in 6 O-Zr/Y-O layers along c for YSZ.

We refer to this model, used throughout all the main text, as $\text{YSZ}^{6\text{L}}\text{-LiKCO}_3^{3\text{L}}$ in the following.

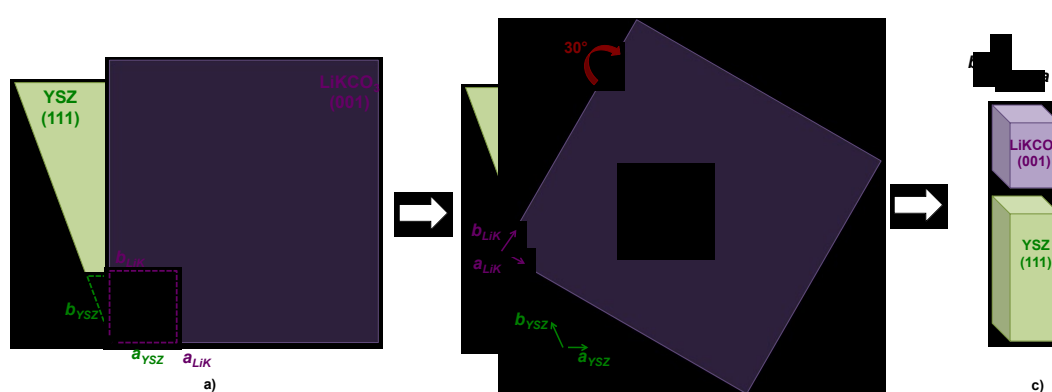


Figure S1: Schematization of the building process of the model YSZ-LiKCO₃ interface considered for all the DFT simulations: a) superposition of a (4×4) supercell of the LiKCO₃-(001) (in violet) and YSZ-(111) (in green) models previously identified; b) rotation of the LiKCO₃-(001) supercell of 30° around the normal to the YSZ-(111) surface plane and identification of a new unit cell for the interface (black dotted line); c) final interface model.

1.2 Alternative interface model

In order to verify the convergence of the interface properties with respect to the thickness of the carbonate layer, we performed auxiliary calculations on a model of the carbonate (001) surface made of 5 slab layers, corresponding to a Li₁₀K₁₀(CO₃)₁₀ stoichiometry for a total of 60 atoms (indicated as LiKCO₃^{5L}). The strategy used to build the interface was the same as the one described above for the other model. However, in order to reduce the computational cost of the calculation, we combined this LiKCO₃^{5L} surface model with a model of YSZ-(001) with just three slab layers (YSZ^{3L}) obtained cutting in half the optimized structure of the oxide in the YSZ^{6L}-LiKCO₃^{3L} interface. The geometry of the as-prepared YSZ^{3L}-LiKCO₃^{5L} model was consequently optimized, allowing to relax the cell parameters and the positions of all the atoms in the carbonate phase, but just the outermost O and Zr/Y atoms of the oxide surface that are directly involved in the interfacial interaction in order to avoid too large deviation from the bulk-like structure of YSZ that can take place considering the reduced thickness of the oxide phase in this model.

2. Results for the alternative interface model

2.1. Results

Figure S1 shows the structure of the optimized YSZ^{3L}-LiKCO₃^{5L} interface model. Also in this case, Li atoms and monodentate and bridged CO₃ are adsorbed on the oxide surface. In order to release the strain due to the lattice mismatch, the carbonate phase shows again a disordered amorphous-like structure, with the carbonate units that change their orientation compared to the initial ordered structure in LiKCO₃-(001) by rigidly rotating mainly about the *b* axis. This perturbation is more important for the atoms closer to YSZ surface and gradually decreases while moving away from it. Values in table S1 confirm this picture, with the unit cell parameters ($a=7.11$ Å, $c=6.25$ Å, $\gamma=90.09^\circ$, and $S=44.45$ Å²), adhesion energy ($E_{\text{ads}}=3.08$ eV and $\beta_{\text{ads}}=0.07$ eV/Å²) and also the band gap (E_g) obtained for this model perfectly in line with the ones of the YSZ^{6L}-LiKCO₃^{3L} model confirming the strong oxide-carbonate interaction and the convergence of the latter model with respect to the thickness of the carbonate phase.

Figure S1: Optimized geometry of the YSZ^{3L}-LiKCO₃^{5L} model of the composite, shown as a (2×2) supercell of the interface model for clarity. Solid blue line indicates the unit cell. Zr, Y, and O atoms are in light blue, green and red, while C, Li and K are in grey, light violet and purple, respectively. Pink small spheres represent the oxygen vacancy positions.

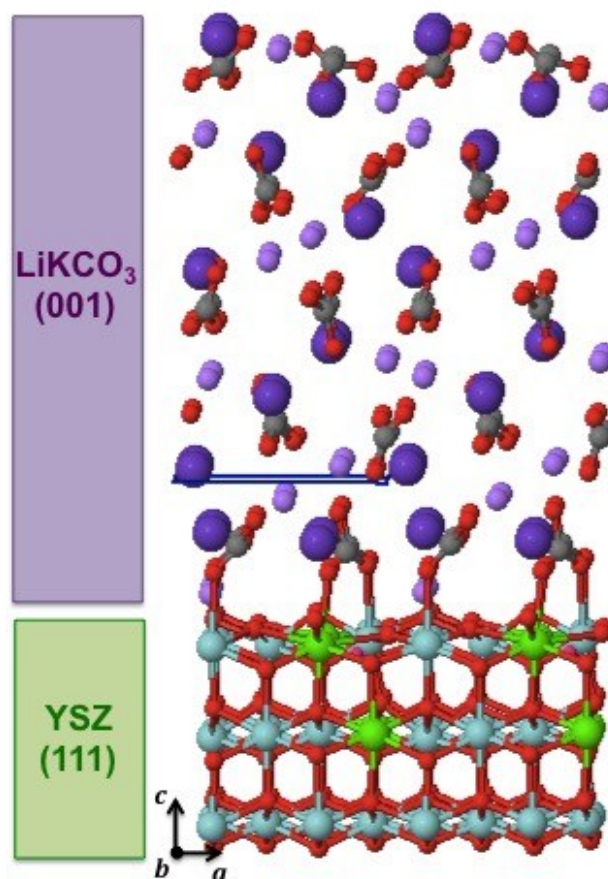


Table S1: Optimized lattice vectors (*a*, *c* in Å), angle (γ , in degrees), and surface area (*S*, in Å²) of the YSZ^{3L}-LiKCO₃^{5L} interface model together with its adhesion energy (*E*_{ads}, in eV), specific adhesion energy (β , in eV/Å²) and optimized band gap (*E*_g, in eV).

References

1. C. Ricca, A. Ringuedé, M. Cassir, C. Adamo and F. Labat, *RSC Adv.*, 2015, **2**, 13941–13951.
2. C. Ricca, A. Ringuedé, M. Cassir, C. Adamo and F. Labat, *Surf. Sci.*, 2016, **647**, 66–77.
3. C. Xia, Y. Li, Y. Tian, Q. Liu, Y. Zhao, L. Jia and Y. Li, *J. Power Sources*, 2009, **188**, 156–162.
4. A. Eichler, *Phys. Rev. B*, 2001, **64**, 174103–8.
5. G. Ballabio, M. Bernasconi, F. Pietrucci and S. Serra, *Phys. Rev. B*, 2004, **70**, 075417–6.
6. A. Christensen and E. Carter, *Phys. Rev. B*, 1998, **58**, 8050–8064.
7. A. Bogicevic, C. Wolverton, G. Crosbie and E. Stechel, *Phys. Rev. B*, 2001, **64**, 014106–14.
8. M. Bruno, M. Rubbo, L. Pastero, F. R. Massaro, F. Nestola and D. Aquilano, *Cryst. Growth Des.*, 2015, **15**, 2979–2987.

YSZ^{3L}- LiKCO₃^{5L}	
<i>a</i>	7.13
<i>c</i>	6.25
γ	90.09
S	44.49
E_{ads}	3.08
β_{ads}	0.07
E_g	5.72